Solid State Communications 250 (2017) 31–34

Contents lists available at ScienceDirect

Solid State Communications

journal homepage: www.elsevier.com/locate/ssc

Communication

# Linear and quadratic magneto-optical Kerr effect investigation of $Co_2Mn_{1.30}Si_{0.84}$ epitaxially grown on MgO

Jihong Liu, Shuang Qiao*, Shufang Wang, Guangsheng Fu

*Hebei Key Laboratory of Optic-Electronic Information and Materials, College of Physics Science and Technology, Hebei University, Baoding 071002, PR China*

ARTICLE INFO

*Keywords:*
Heusler alloy
Half-metal
Magnetic anisotropy
Quadratic magneto-optical Kerr effect

ABSTRACT

We investigated the magneto-optical properties of a $L2_1$ ordered nonstoichiometric $Co_2Mn_{1.30}Si_{0.84}$ film epitaxially grown on a MgO-buffered MgO (001) single-crystal substrate. Longitudinal magneto-optical Kerr effects (LMOKE) and rotating magneto-optical Kerr effect (ROT-MOKE) measurements suggest that the film exhibits a cubic magnetic anisotropy with the extracted cubic anisotropy constant of $K_C = 6.7 \times 10^4 erg/cm^3$. Orientation-dependent ROT-MOKE suggest that the quadratic magneto-optical Kerr effects (QMOKE) components also show fourfold symmetry with a modest amplitude of 3 mdeg, which is in accordance with complex Kerr angle expression for cubic symmetry systems. Our results suggest that ROT-MOKE is not only an efficient method to determine magnetic anisotropy parameters but also a good method to extract QMOKE components.

## 1. Introduction

Half-metallic ferromagnets (HFMs) are respected as one of the ideal materials in spintronics, such as spin transport-based electronics, spin injection sources, as they are predicted to exhibit 100% spin polarization at the Fermi level [1,2]. Among different HMFs the Heusler alloy $Co_2MnSi$ (CMS) has attracted particular interest, especially when an exceptionally large spin polarization of about 97% was observed directly in experiment at room temperature [3]. The Fermi level of CMS lies near the middle of the minority spin band gap (about 0.4–0.8 eV) [2,4]. This is advantageous for conserving half-metallicity at finite temperatures or in the presence of defects which smear the electron density near the valence or conduction bands. Furthermore, CMS boasts a very high Curie temperature of 985 K [5], which is a prerequisite for implementation in practical devices. Besides, it also features a small lattice mismatch of about −5.4% between $Co_2MnSi$ [100] orientation and MgO [110] orientation in the (001) plane [6]. This small mismatch is not only preferable for realizing high-performance magnetic tunnel junctions (MTJs) with potentially half-metallic Heusler-compound electrodes, but also to build layered structures for spin-injection from a Heusler-compound electrode into semiconductors through a MgO barrier.

Till now, the structure, magnetic, electronic properties of Co-based Heusler alloy have been investigated by many groups [6–12], it is well accepted that most of these alloys show strong quadratic magneto-optical Kerr effects (QMOKE). This effect was first seen in $Co_2FeSi$ film [7], which is the largest ever reported, then it was boosted in $Co_2MnGe$ [6,8,9], $Co_2MnSi$ [10,11], $Co_2FeSi_{0.5}Al_{0.5}$ [12]and also in other ferromagnetic metals [13,14]. In 2002, this effect has been given a phenomenological explanation by Postava et al., and was also believed to be directly related to spin orbit coupling [15,16]. It is well known that most of magnetic properties was related to spin-orbit interaction, such as magnetic anisotropy [17], magnetic damping [18]and so on. Therefore, considering the possible correlation between these magnetic properties, it is fundamentally important to study this effect.

Up to date, QMOKE can be investigated experimentally by longitudinal magneto-optical Kerr effect (LMOKE) with perpendicular laser incident or dual-beam MOKE magnetometer [10]. However, these measurements usually need a four pole magnet, which is used to provide in-plane magnetic field along different orientations. While, since 1999, R. Mattheis and G. Quednau [19] found a new method to study magnetic anisotropy constants of the thin films by combining both rotating field orientation and LMOKE, which is called as rotating magneto-optical Kerr effect (ROT-MOKE), ROT-MOKE was considered to be an efficient method to determine magnetic anisotropy parameters. However, besides getting magnetic anisotropy parameters, ROT-MOKE may be still a very convenient method to determine QMOKE by combining both ROT-MOKE and rotating film orientation.

* Corresponding author.
*E-mail address:* sqiao@hbu.edu.cn (S. Qiao).

http://dx.doi.org/10.1016/j.ssc.2016.10.016
Received 26 August 2016; Accepted 31 October 2016
Available online 11 November 2016

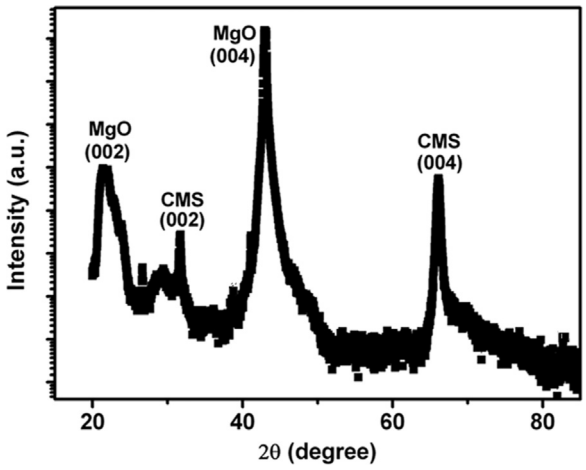


**Fig. 1.** XRD result of 30 nm-thick $Co_2Mn_{1.30}Si_{0.84}$ film annealed at 873 K.

## 2. Sample preparation and structural characterization

In this work, we carried out the LMOKE, ROT-MOKE and QMOKE measurements for CMS film. The MOKE measurements were performed using a He-Ne laser with a wavelength of 632.8 nm. During the measurement, a linear s-polarized laser is incident on the film surface, and reflected from it, and then passes through a polarization analyzer with 2° offset from extinction and at last measured by a photodiode. The Kerr rotation angle can be quantitatively determined as illustrated in Ref. [20].

The film was epitaxially grown on MgO (001) substrate with thickness of 30 nm by radio frequency magnetron sputtering at room temperature (RT), and subsequently annealed *in situ* at 873 K. Finally, a 2 nm-thick aluminum layer was deposited by current sputtering at RT and a native oxide was formed in an oxygen atmosphere over a period of 2 h. Further details of the sample preparation can be found in Ref. [21].

X-ray diffraction measurement result was shown in Fig. 1, from which we can clearly observe [002] and [004] reflection peak, indicating perfect epitaxial [100] growth. A cross-sectional high-resolution transmission electron microscope (HR-TEM) measurements also revealed that CMS films were epitaxially grown on MgO substrate [22,23]. Furthermore, the (111) diffraction spots were also observed by electron diffraction, which suggest that the film is at least partially $L2_1$ ordering [22]. Using inductively coupled plasma optical emission spectroscopy, the composition of a thin film prepared under the same condition was determined to be $Co_2Mn_{1.30}Si_{0.84}$, with an accuracy of 2–3% for each element.

## 3. Results and discussions

The hysteresis loops and coercivity of different in-plane orientations were studied by LMOKE, with external magnetic field being applied in-plane and parallel to the plane of light incidence. All the measurements were investigated at room temperature by s-polarized laser with wavelength of 633 nm and an angle of incidence of 45°, the sketch of which was shown in Fig. 2. The MOKE hysteresis loops at various orientation $\varphi$ between the [110] axis and magnetic field H are measured with rotating steps of 5° or 10°, and three typical loops with magnetic field H applied along [110], [100] and [1̄10] directions are shown in Fig. 3(a). The deduced orientation-dependent coercivity was shown in Fig. 3(b), from which one can observe clear four-fold symmetry, suggesting that this CMS has cubic anisotropy with easy axis along in-plane (110) orientation and hard axis along in-plane (100) orientation.

In order to determine the cubic anisotropy constant $K_C$, a more economic way is to fit the magnetization loop with an analytic

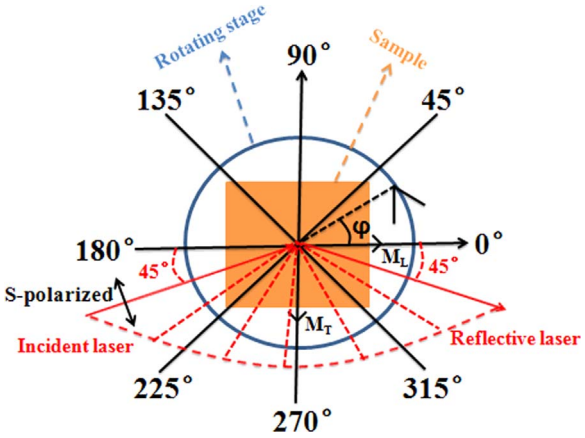


**Fig. 2.** Optical geometry, sample rotation and in-plane field directions used for MOKE measurements.

expression. If an applied field is much larger than saturated field, the film will be in a single-domain state, which is allowed a simple mathematical description of the magnetization rotation. Assuming a magnetization process by reversible rotation, an analytic expression can be obtained by minimizing the magnetic energy density $\varepsilon(\varphi_M)$ as follows [19,24,25]:

$$\frac{\partial \varepsilon(\varphi_M)}{\partial \varphi_M} = -\frac{1}{2}K_C \sin(4\varphi_M) + HM_S \sin(\theta_H - \varphi_M) = 0 \Leftrightarrow$$
$$HM_S \sin(\theta_H - \varphi_M) = \frac{1}{2}K_C \sin(4\varphi_M) \quad (1)$$

where $\theta_H$ is the angle between the in-plane external field and the [110] axis, $\varphi_M$ is the angle between the magnetization and [110] axis; $K_C$ is the cubic anisotropy constant; and $M_S$ is the saturation magnetization. Therefore, the only problem for the determination of $K_C$ is to determine the angle $\varphi_M$ corresponding to each $\theta_H$. In Eq. (1), the term of $l(\varphi_M) = HM_S \sin(\theta_H - \varphi_M)$is a torque, which is usually determined by the torquemeter [26].

However, for the investigated system with a cubic symmetry, a (100) interface plane and s-polarized laser, the complex Kerr angle is given by [16]:

$$\Phi_{Kerr} = AKM_L + BM_LM_T + C(M_L^2 - M_T^2) \quad (2)$$

where $A$ is the optical weighting factor, $K$ is the linear magneto-optical constant, $B = \beta[(-\frac{K^2}{n^2} + 2G_{44} + \frac{\Delta G}{2} - \frac{1}{2}\Delta G \cos(4\phi)]$ and $C = \frac{1}{4}\Delta G \sin(4\phi)$, $\beta$ is also the optical weighting factor, $\Delta G = G_{11} - G_{12} - 2G_{44}$, with $G_{11}$, $G_{12}$, and $G_{44}$ being the remaining elements of the quadratic magneto-optical tensor, and $n$ is the complex refractive index of the material. The angle $\phi$ is the orientation of the crystallographic axes with respect to the plane of incidence (here $\phi = 0^\circ$ is defined as [110] orientation). From Eq. (2), we can observe that the total Kerr signal comes from three different contributions, which can be explained as: (1) The first term describes the linear contribution proportional to $M_L$; (2) The second and third terms are the QMOKE contributions, proportional to $M_LM_T$ and $M_L^2 - M_T^2$ respectively. It is obvious that only the QMOKE contributions depend on the sample orientation and on the value of $\Delta G$. So that the various components of the signal can be separately evaluated for a given in-plane orientation $\phi$ by measuring the Kerr rotation $\Phi_{Kerr}$ in saturation for eight in-plane field orientations as following [7,16],

$$\Phi_{M_L}^{sat} = \frac{1}{2}[\Phi_{0^\circ} - \Phi_{180^\circ}] \quad (3)$$

$$\Phi_{M_LM_T}^{sat} = \frac{1}{4}[\Phi_{45^\circ} + \Phi_{225^\circ} - \Phi_{135^\circ} - \Phi_{315^\circ}] \quad (4)$$

$$\Phi_{M_L^2 - M_T^2}^{sat} = \frac{1}{4}[\Phi_{0^\circ} + \Phi_{180^\circ} - \Phi_{90^\circ} - \Phi_{270^\circ}] \quad (5)$$

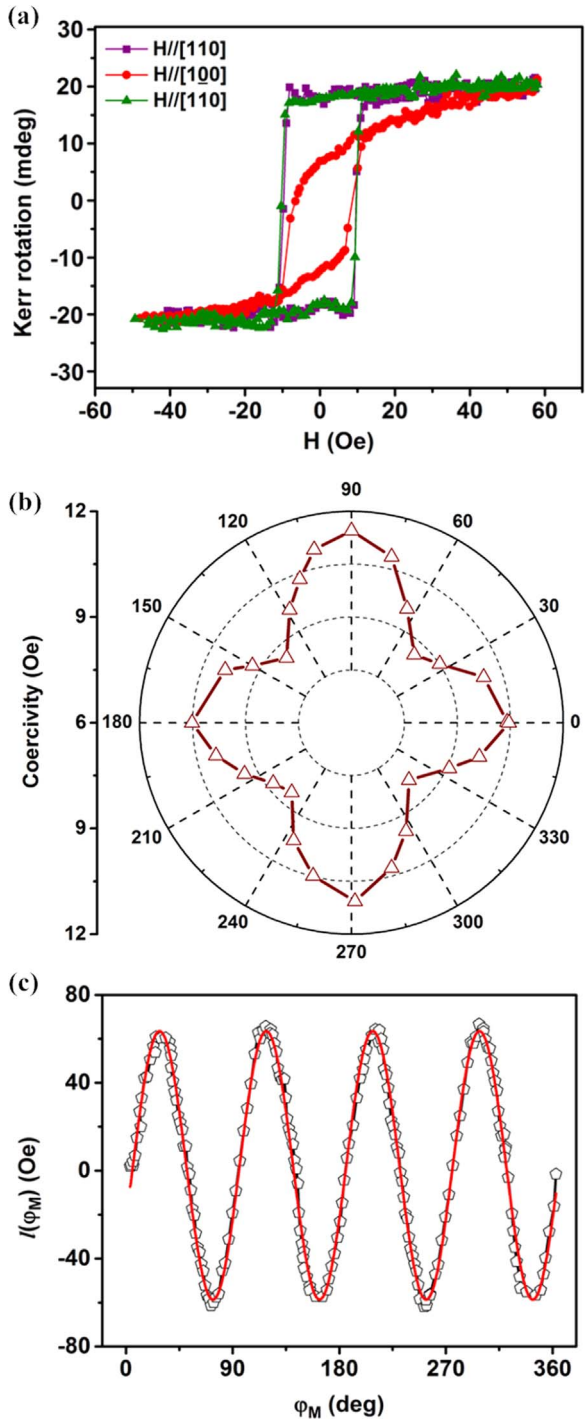


**Fig. 3.** (a) Longitudinal MOKE hysteresis loops measured at in-plane [110], [100] and [110] orientations. (b) The angular dependence of in-plane magnetic coercive field. (c) The measured ROT-MOKE curve and its best fitting (red solid line) for $Co_2Mn_{1.30}Si_{0.84}$ film.

where the subscripts correspond to the in-plane directions of the applied field generated by a four poles electric magnet as shown in Fig. 2.

From Eq. (3), the linear part $\Phi_{M_L}^{sat}(\theta_H)$, which allows one to determinate the angle $\varphi_M$ by solving $M_L(\varphi_M) = M_S \cos\varphi_M$, can be gotten [19]. Then, by employing ROT-MOKE with very large applied filed of 1000 Oe, we can simultaneously determine the two angles $\theta_H$ and $\varphi_M$. Fig. 3(c) gives the ROTMOKE curve of CMS, which can be very well fitted by $I(\varphi_M) = \frac{1}{2}K_C \sin(4\varphi_M)$, with the extracted cubic anisotropy constant to be $K_C = 6.7 \times 10^4 \mathrm{erg/cm^3}$, also suggesting that the CMS film shows only the cubic anisotropy.

Moreover, from Eq. (2), we can observe that the measured Kerr signal is contributed by both the LMOKE and QMOKE, so that the measured MOKE hysteresis curve may exhibit an asymmetry with respect to an inversion of the magnetic field. As can be seen in Fig. 4(a), a typical asymmetry was obtained at an in-plane orientation of 55°. The symmetric and asymmetric components of the Kerr signal $\Phi_{Kerr}$ can be extracted by following methods [7,10]:

$$LMOKE_{\uparrow\downarrow} \mapsto \Phi_{sym} = \frac{\Phi(H_{\uparrow\downarrow}) - \Phi(-H_{\downarrow\uparrow})}{2} \tag{6}$$

$$QMOKE_{\uparrow\downarrow} \mapsto \Phi_{asym} = \frac{\Phi(H_{\uparrow\downarrow}) + \Phi(-H_{\downarrow\uparrow})}{2} \tag{7}$$

where the arrows ↑ and ↓ indicate the branches of the loop with increasing and decreasing field strengths, respectively. The extracted symmetry component is attributed to the LMOKE, as shown in Fig. 4(a), and the extracted asymmetry component to the QMOKE, as shown in Fig. 4(b).

To quantify the contributions of the QMOKE components, the ROT-MOKE loops at various in-plane orientations $\varphi$ are measured with rotating steps of 5° and very large field of 1000 Oe, then, we can get the linear contribution and QMOKE contributions by extracting the Kerr signal of these eight directions for every in-plane orientation through Eqs. (4) and (5), respectively. In order to improve the ratio of signal to noise, we got the ROT-MOKE loop by averaging several rotating circles for every in-plane orientation. Fig. 5 displays the angular dependence of the LMOKE and QMOKE signals at incident angle of 45°. It is clearly observed that the LMOKE signal $AKM_L$ is independent of $\varphi$. On the other hand, the QMOKE signal that related to $C(M_L^2 - M_T^2)$, is proportional to $\sin(4\varphi)$, whereas the QMOKE signal that related to $BM_LM_T$, is proportional to $\cos(4\varphi) + D$, with $D$ a constant, suggesting the results are in accordance with Eq. (3). Although some researchers reported that the QMOKE may be related to the spin-orbit coupling and electron transitions [15,16], the origin of it is still not fully understood. Till now, it is assumed that QMOKE components observed among different films of cubic symmetry systems (such as $Co_2FeSi$ [7], $Co_2Mn_xGe_{2-x}$ [6,8,9], $Co_2MnSi$ [10,11], Fe [13–15]and so on) shows the similar fourfold symmetry, only with different amplitude and intercept. Here, for this CMS film, ROT-MOKE measurements indicate that not only the QMOKE shows fourfold symmetry, but also the magnetic anisotropy shows fourfold symmetry, which is different from that of $Co_2Mn_{0.77}Ge_{0.42}$ film [6].

## 4. Conclusion

In summary, we investigated the $L2_1$ ordered $Co_2MnSi$ film by means of LMOKE, ROT-MOKE, and QMOKE. We find that the film exhibits a cubic magnetic anisotropy with $K_C = 6.7 \times 10^4 \mathrm{erg/cm^3}$. A modest QMOKE with an amplitude of 3 mdeg is obtained. Moreover, as is described by Kerr angle expression for cubic symmetry systems, both magnetic anisotropy and QMOKE components behave the similar fourfold symmetry. Our results suggest that ROT-MOKE can be used to determine both magnetic anisotropy and QMOKE components.

## Acknowledgments

This work was supported in part by the National Natural Science Foundation of China (Grant nos. 11504076 and 51372064), in part by the One Hundred Talent Project of Hebei Province (Grant no. E201300013), in part by the Science and technology research project of higher education institution of Hebei Province (Grant no. ZD2016036), in part by the Second Batch of Young talents of Hebei Province, and in part by Nature Science Foundation for Distinguished Young Scholars of Hebei University (Grant no. 2015JQ03). The authors thank Yusuke Honda and Masafumi Yamamoto (Hokkaido University,

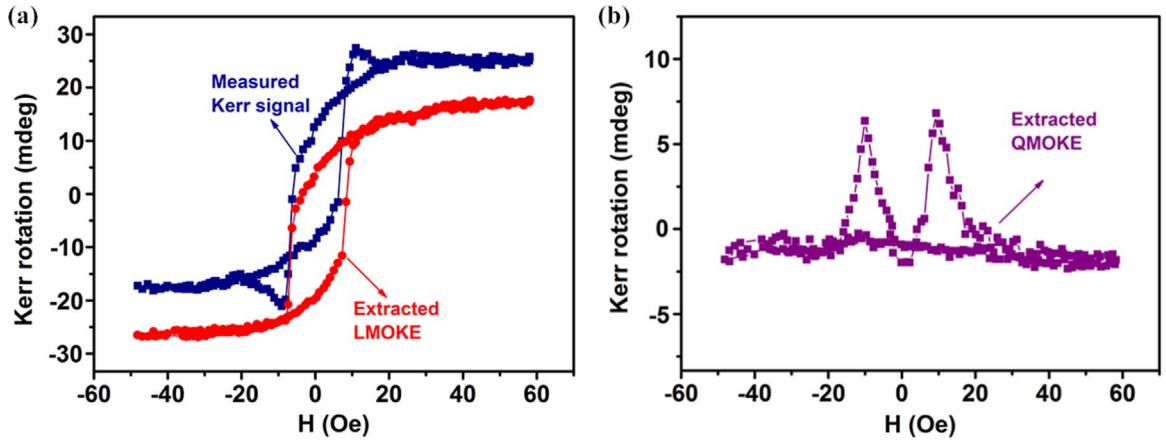


**Fig. 4.** (a) Hysteresis loops measured by MOKE at sample orientation of $\varphi = 55^{\circ}$ (black dots line) as well as the extracted longitudinal MOKE (red dots line). (b) The extracted quadratic MOKE components of the signal. (For interpretation of the references to color in this figure legend, the reader is referred to the web version of this article.).

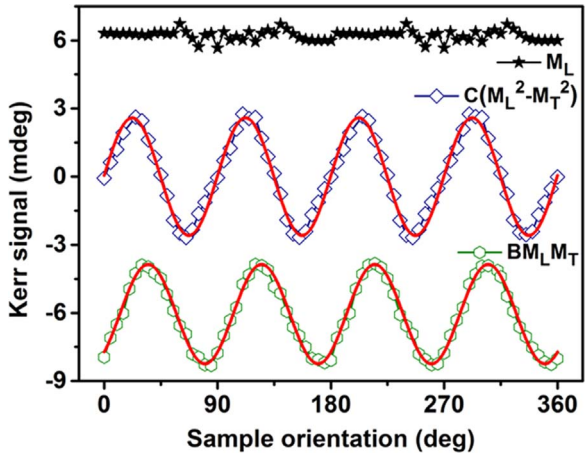


**Fig. 5.** The separated QMOKE contributions as a function of the sample in-plane orientation $\varphi$: $AKM_L$ contribution (black stars), $C(M_L^2 - M_T^2)$ contribution (blue squares), $BM_L M_T$ contribution (green circles), with red fitting lines as expressed in Eq. (2). (For interpretation of the references to color in this figure legend, the reader is referred to the web version of this article.).

Japan) for providing the sample.

## References

[1] I. Galanakis, P.H. Dederichs, N. Papanikolaou, Phys. Rev. B 66 (2002) 174429.
[2] S. Picozzi, A. Continenza, A.J. Freeman, Phys. Rev. B 66 (2002) 094421.
[3] M. Jourdan, J. Minar, J. Braun, A. Kronenberg, S. Chadov, B. Balke, A. Gloskovskii, M. Kolbe, H.J. Elmers, G. Schonhense, H. Ebert, C. Felser, M. Klaui, Nat. Commun. 5 (2014) 3974.
[4] S. Fujii, S. Sugimura, S. Ishida, S. Asano, J. Phys.: Condens. Matter 2 (1990) 8583.
[5] P.J. Brown, K.-U. Neumann, P.J. Webster, K.R.A. Ziebeck, J. Phys.: Condens. Matt. 12 (2000) 1827.
[6] S. Trudel, J. Hamrle, B. Hillebrands, T. Taira, M. Yamamoto, J. Appl. Phys. 107 (2010) 043912.
[7] J. Hamrle, S. Blomeier, O. Gaier, B. Hillebrands, H. Schneider, G. Jakob, K. Postava, C. Felser, J. Phys. D: Appl. Phys. 40 (2007) 1563.
[8] P.K. Muduli, W.C. Rice, L. He, F. Tsui, J. Magn. Magn. Mater. 320 (2008) L141.
[9] P.K. Muduli, W.C. Rice, L. He, B.A. Collins, Y.S. Chu, F. Tsui, J. Phys.: Condens. Matt. 21 (2009) 296005.
[10] S. Trudel, G. Wolf, H. Schultheirb, J. Hamrle, B. Hillebrands, T. Kubota, Y. Ando, Rev. Sci. Instrum. 81 (2010) 026105.
[11] G. Wolf, J. Hamrle, S. Trudel, T. Kubota, Y. Ando, B. Hillebrands, J. Appl. Phys. 110 (2011) 043904.
[12] S. Trudel, G. Wolf, J. Hamrle, B. Hillebrands, P. Klaer, M. Kallmayer, H.-J. Elmers, H. Sukegawa, W. Wang, K. Inomata, Phys. Rev. B 83 (2011) 104412.
[13] M. Buchmeier, R. Schreiber, D.E. Burgler, C.M. Schneider, Phys. Rev. B 79 (2009) 064402.
[14] J.H. Liang, X. Xiao, J.X. Li, B.C. Zhu, J. Zhu, H. Bao, L. Zhou, Y.Z. Wu, Opt. Express 23 (2015) 11357.
[15] K. Postava, D. Hrabovský, J. Pištora, A.R. Fert, Š. Višňovský, T. Yamaguchi, J. Appl. Phys. 91 (2002) 7293.
[16] R.M. Osgood III, S.D. Bader, B.M. Clemens, R.L. White, H. Matsuyama, J. Magn. Magn. Mater. 182 (1998) 297.
[17] K. Garello, I.M. Miron, C.O. Avci, F. Freimuth, Y. Mokrousov, S. Blugel, S. Auffret, O. Boulle, G. Gaudin, P. Gambardella, Nat. Nanotechnol. 8 (2013) 587–593.
[18] P. He, X. Ma, J.W. Zhang, H.B. Zhao, G. Lupke, Z. Shi, S.M. Zhou, Phys. Rev. Lett. 110 (2013) 077203.
[19] R. Matteis, G. Quednau, J. Magn. Magn. Mater. 205 (1999) 143–150.
[20] Z.Q. Qiu, S.D. Bader, Rev. Sci. Instrum. 71 (2000) 1243.
[21] G.H. Fecher, B. Balke, A. Gloskowskii, S. Ouardi, C. Felser, T. Ishikawa, M. Yamamoto, Y. Yamshita, H. Yoshikawa, S. Ueda, K. Kobayashi, Appl. Phys. Lett. 92 (2008) 193513.
[22] T. Ishikawa, T. Marukame, H. Kijima, K.I. Matsuda, T. Uemura, M. Yamamoto, Appl. Phys. Lett. 89 (2006) 192505.
[23] H. Kijima, T. Ishikawa, T. Marukame, H. Koyama, K. Matsuda, T. Uemura, M. Yamamoto, IEEE Trans. Magn. 42 (2006) 2688.
[24] S. Qiao, S.H. Nie, J.H. Zhao, X.H. Zhang, J. Appl. Phys. 113 (2013) 233914.
[25] S. Qiao, S.H. Nie, J.H. Zhao, X.H. Zhang, J. Appl. Phys. 117 (2015) 093904.
[26] F.B. Humphrey, A.R. Johnston, Rev. Sci. Instrum. 34 (1963) 348.